Progress In Electromagnetics Research, Vol. 176, 45–53, 2023

Commercial-Printed-Circuitry-Compatible Self-Superhydrophobic Antennas Based on Laser Direct Writing

Xiao-Liang Ge[1, #], Jun-Hao Yang[1, #], Hang Ren[1], Zhi-Jun Qin[1], Qi-Dai Chen[1], Dong-Dong Han[1, *], Yong-Lai Zhang[1, *], Su Xu[1, *], and Hong-Bo Sun[1, 2]

Abstract—Antennas are essential devices to build everything connected in the era of information. However, the quality of communications would be degraded with the presence of raindrops on the antenna surface. Additional antiwater radomes may generate radiation loss and dispersive impedance mismatch over a broad frequency range, which is not acceptable for next-generation communication systems integrating multiple bands. Here, we report the first experimental demonstration of self-hydrophobic antennas that cover the bands of 1.7 GHz, 3.5 GHz, and 8.5 GHz through a laser-direct-writing treatment. Experimental results show that the return loss, radiation pattern, and efficiency of self-superhydrophobic antennas can be maintained in the mimicked rainy weather. Furthermore, writing hydrophobic nanostructures on both dielectrics and metals is compatible with commercial printed circuitry techniques widely used in industries. Our technique will augment the laser fabrication technology for specialized electromagnetic devices and serve as a powerful and generalized solution for all-weather wireless communication systems.

1. INTRODUCTION

In the current information age, wireless communication makes everyone and everything connected. Antennas have been widely used in almost all areas of the current information world, much like the human eyes and ears, because antennas can convert free-space electromagnetic waves in wireless channels to currents (or guided mode) in transmission line circuits, and vice versa [1–5]. The impedance matching condition [6–9] at the radiation interface established by the antennas and the surroundings, which is generally pre-designed, determines the conversion efficiency (Fig. 1(a)). However, the pre-defined impedance matching condition may worsen in particular adverse environments (e.g., days of heavy/frozen rain) (Fig. 1(b)). Such environment-related impedance mismatch will introduce unnecessary spectral shifts and radiation loss, which are obstacles to all-weather wireless communication [10–14].

Additional radomes have been employed in antenna systems to remove the liquid surface from antennas. The majority of modern radomes are made of thin dielectric coatings [15–18] or artificial electromagnetic structures [19–22] to melt snow, evaporate water or let water fall from Radomes, as a component of the transmission line of a well-designed antenna system may successfully perform impedance matching within a suitable frequency band but will introduce dispersive impedance mismatch over broad frequency bands where the wavelengths differ by order. This dispersive impedance mismatch will result in greater return loss, worse radiation efficiency, and a shorter transmissive range. None of

Received 11 October 2022, Accepted 17 November 2022, Scheduled 28 November 2022

* Corresponding authors: Dong-Dong Han (handongdong@jlu.edu.cn), Yong-Lai Zhang (yonglaizhang@jlu.edu.cn) and Su Xu (xusu@jlu.edu.cn). # These authors contributed equally to this work.

[1] State Key Laboratory of Integrated Optoelectronics, College of Electronic Science and Engineering, Jilin University, Changchun 130012, China. [2] State Key Laboratory of Precision Measurement Technology and Instruments, Department of Precision Instrument, Tsinghua University, Haidian, Beijing 100084, China.

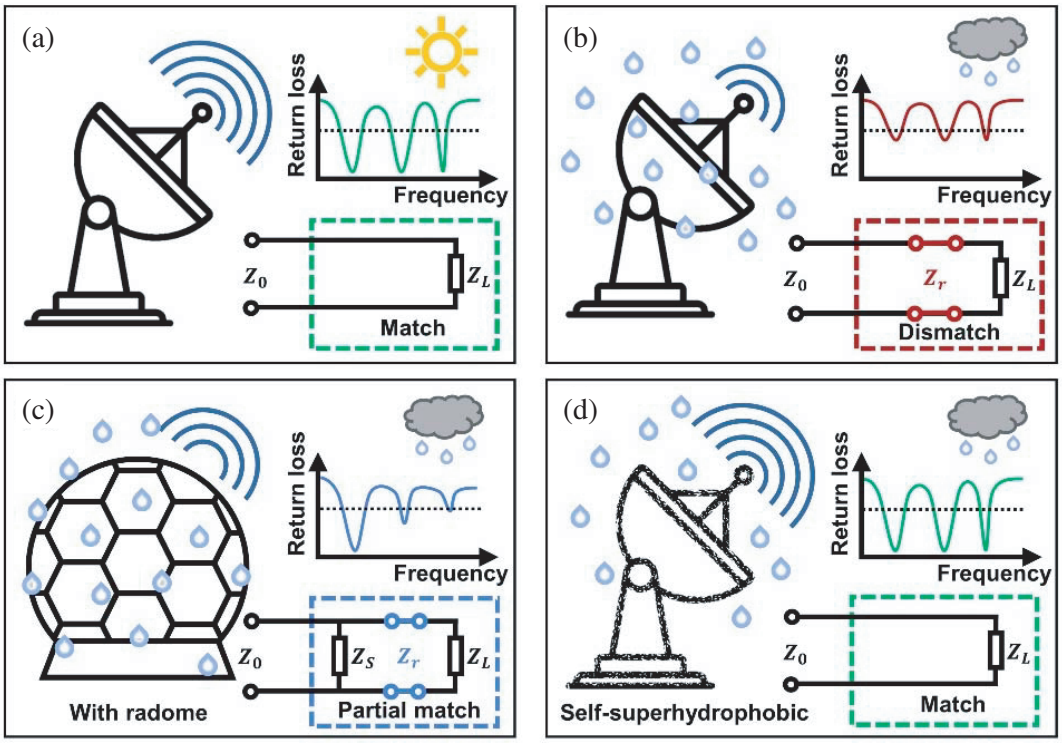

Figure 1. (a) Conventional antenna. (b) Conventional antenna in the rain. (c) Antenna with radome in the rain. (d) Self-superhydrophobic antenna in the rain.

these degradations on antenna performance are acceptable for next-generation wireless communication systems integrating sub-6 GHz to higher frequencies (Fig. 1(c)).

In this work, we report a novel laser-direct-writing method for self-superhydrophobic radio-frequency devices (Fig. 1(d)). This technique will enable the production of hydrophobic microstructures inspired by butterfly wings on the metallic patterns and dielectric substrates of ordinary printed circuit boards (PCB). Optical microscopy techniques are used to explain the geometrical characteristics and hydrophobicity of bioinspired microstructures. The reported work is also the first experimental demonstration of a self-superhydrophobic antenna for multiband radiation, to the best of our knowledge. It has been observed that the self-superhydrophobic antenna's surface was impervious to raindrops. The proposed laser-writing treatment can achieve hydrophobic microstructures on both dielectric substrates and antenna patterns. Therefore, the proposed method is compatible with the commercially printed circuitry technique that is widely used in industries and can be used as a potent tool for Beyond-5G multiband-integrated all-weather wireless communication systems. This research also points to a new field of research toward the manufacturing of unique electromagnetic gadgets using cutting-edge laser technology.

2. RESULTS AND DISCUSSION

2.1. Laser Direct Writing Treatment for Superhydrophobic Application

In nature, butterfly wings consist of longitudinal ridges, lateral bridges, and nano stripes of multiple dimensions (Fig. 2(a) [23]). These organs greatly reduce the contact area between water droplets and wing surfaces and achieve hydrophobicity. Inspired by butterflies, to artificially realize the micro-scale geometrical characteristic of this amazing hydrophobic organism, an efficient way is laser direct writing technique. For instance, Prof. Deng and his team show that robust superhydrophobicity can be realized by structuring surfaces at two different length scales by laser direct writing [24]. The schematic view of the fabrication process is illustrated in Fig. 2(b). A FOTIA UV laser processor with the average

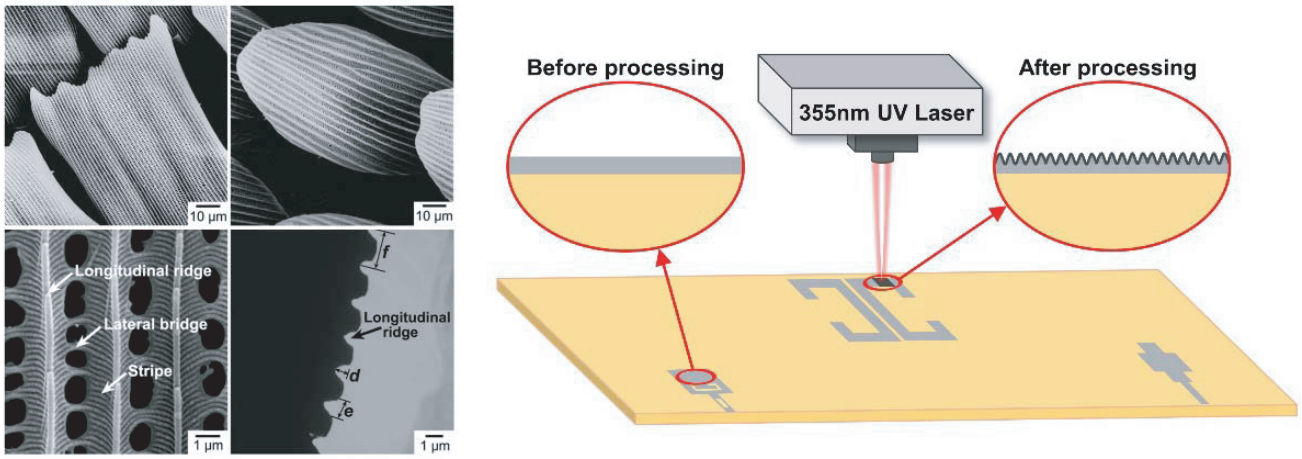

(a) (b)

Figure 2. (a) The bio-inspiration of nanostructure: wings of butterfly. The photo is reproduced from [23], used with permission. (b) The schematic view of laser processing for self-superhydrophobic antennas.

power of 3 W (at 355 nm wavelength) and the repetition rate of 30 kHz is used to obtain artificial grooved structures [25–39]. The line spacing used in the fabrication is 50 μm. After laser direct writing treatment, both the metallic and dielectric surfaces of antennas are treated with 1H, 1H, 2H, 2H-perfluorodecyltriethoxysilane in an oven at 96°C for 10 hours.

The hydrophobicity and microscale surfaces of copper and FR-4 (Flame Retardant-4, glass fiber epoxy resin poly dielectric substrate) substrate are characterized experimentally. The relationships between the contact angle and laser scanning speed of copper and FR-4 substrate are illustrated in Fig. 3(a). Since the contact angles should be as large as possible for achieving hydrophobicity, the optimized scanning speeds are selected as 5 mm/s and 70 mm/s for the cases of copper and FR-4 substrate, respectively. With the optimized fabrication parameters mentioned above, the laser-treated copper and FR-4 surface exhibit excellent contact angles of $161 \pm 2°$ and $158 \pm 2°$, respectively, both of which are larger than the critical value of superhydrophobicity for water. Therefore, waterdrops can stand on the treated metallic and dielectric surfaces as shown in Figs. 3(b) and 3(c). Additionally, the microscopic geometries of the fabricated hydrophobic structures are characterized with the use of a super depth of field 3D microscopy system. One can see that both the metallic (Fig. 3(d)) and dielectric (Fig. 3(e)) hydrophobic structures own grooved surfaces, just like butterflies' wings shown in Fig. 2(a). These microscopic geometries and corresponding characterizations indicate that the proposed laser direct writing process can generate hydrophobic surfaces on both metallic and dielectric surfaces. Additionally, it is possible to integrate necessary laser equipment with current commercial PCB machines. Our treatment is also feasible for a large-scale metasurface antenna by dividing the fabrication area into several segments. For instance, a rough duration estimation of fabricating 0.5 m × 0.5 m metasurface antenna [40] is about 62 hours.

2.2. Antenna Design

We design a multi-band antenna for the proof of concept, as shown in Fig. 4(a). The proposed antenna is composed of three distinct antenna unit cells. They are, a dipole antenna, a monopole antenna and a slot antenna, whose center frequencies are 1.7 GHz, 3.5 GHz, and 8.5 GHz, respectively. In the following part of paper, we number the dipole, monopole and slot antenna as Antenna 1, Antenna 2, and Antenna 3 respectively. A FR-4 substrate ($\varepsilon_r = 4.3$, $\tan\delta = 0.009$, 220 mm × 120 mm × 2 mm) was employed. Fig. 4(b) presents the simulated return loss and efficiency of the antenna. One can see that the antenna elements match well with the free space or sunny days. In such an ideal working environment, the efficiencies of each antenna element reach 91%, 87% and 71% at their corresponding

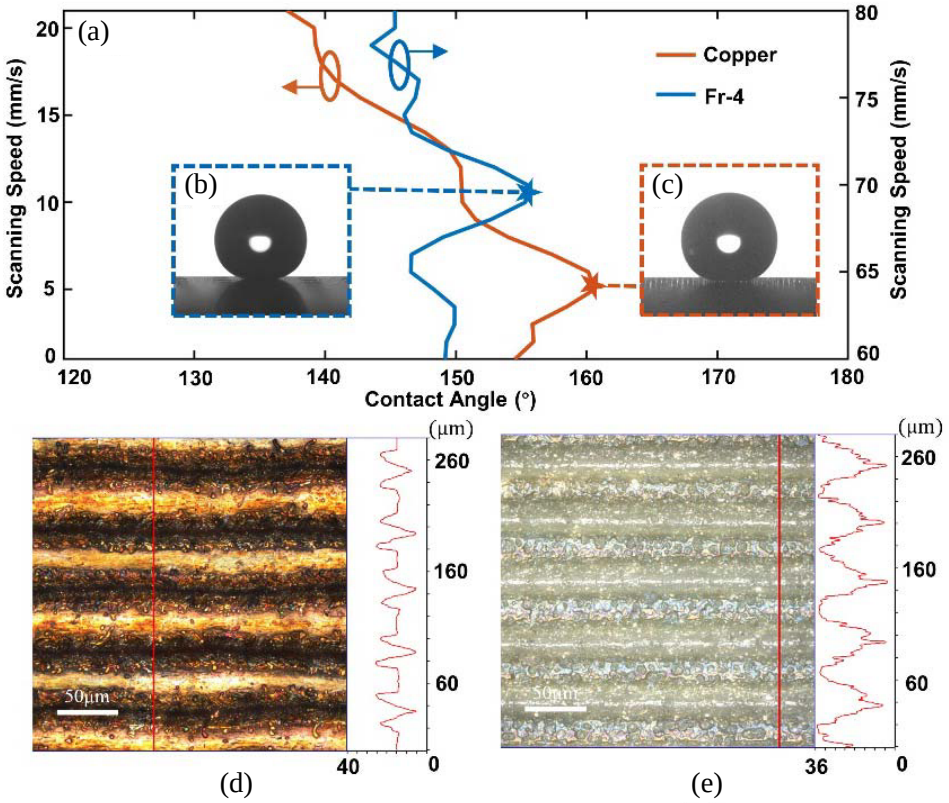

Figure 3. (a) Relationship between the contact angle and laser scanning speed. (b) and (c) The contact angle of superhydrophobic copper and FR-4 surface, respectively. (d) Surface topography of copper after laser direct writing. (e) Surface topography of FR-4 after laser direct writing.

center frequencies respectively. Additionally, the E-plane and H-plane radiation patterns of all the antenna elements are also plotted in Figs. 4(c) and 4(d) for reference.

2.3. Experimental Verification of Superhydrophobic Antenna

In the practical proof of concept, the antenna is firstly fabricated with the typical PCB technique by employing Shanghai Jiajietong Circuit Technology Co. Ltd. Each antenna unit cell is connected to a 50 Ω SMA connector located on the bottom surface of the FR4 substrate. The measurement is carried out in the microwave chamber with a SATIMO SG Antenna Test System, as shown in Fig. 5(a).

In the experiments, we first spray water onto the surfaces of both conventional and hydrophobic antennas to study the hydrophobicity of practical antenna in the mimicked rainy environment. For the case of conventional PCB antenna as shown in Fig. 5(b), water flow spreads over the antenna surface, holds on the surface and form a layer of water thin film (Fig. 5(c)). In contrast, water flow bounces off from the superhydrophobic surface (Fig. 5(d)) and no water film holds on the antenna surface (Fig. 5(e)) for the case of superhydrophobic antenna. The water-spraying experiment indicates an excellent hydrophobic ability of the laser-treated practical PCB antenna. More information on the water spraying experiment can be found in the supplementary movies.

Then, the electromagnetic characteristics of antennas are studied experimentally. For the case of conventional PCB antenna, the return loss deteriorates seriously after spraying water and the working frequency bands occur significant red shift due to the existence of water film, as shown in Fig. 6(a). Consequently, as shown in Fig. 6(c), the efficiency of conventional PCB antennas in the mimicked rainy days (i.e., after spraying water) decrease by more than 20% compared to the case of mimicked sunny days (i.e., before spraying water). Additionally, Figs. 6(e), (f), (i), (j) show that radiation patterns of

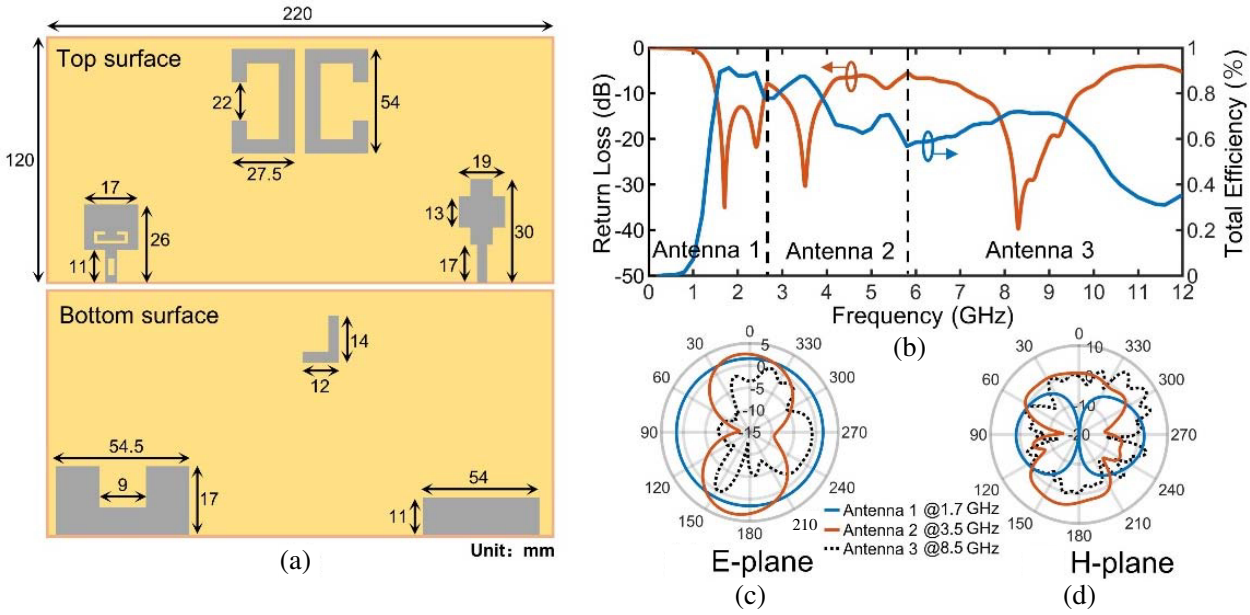

Figure 4. (a) The schematic view of multiband antenna for proof of concept. (b) The simulated return loss and total efficiency. (c) and (d) The simulated radiation pattern of antenna 1, antenna 2 and antenna 3, respectively.

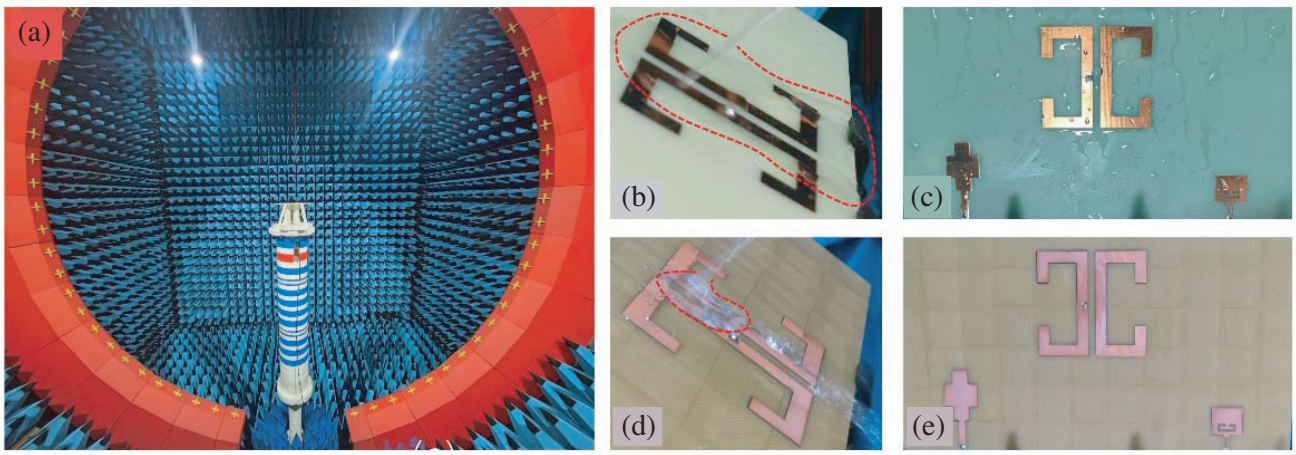

Figure 5. (a) Antenna test environment. (b) Water spreads on the surface of conventional antenna during spraying. (c) Water stays on the surface of conventional antenna after spraying. (d) Water bounces off from the superhydrophobic surface during spraying. (e) No water stays on the superhydrophobic surface after spraying.

conventional metallic antennas are seriously deformed in the mimicked rainy days. All these phenomena indicate that the conventional PCB antenna cannot perform its functionality perfectly in rainy days. However, for the case of self-superhydrophobic antenna, all the key performances including return loss (Fig. 6(b)), efficiency (Fig. 6(d)) and radiation patterns of antenna elements (Figs. 6(g), (h), (k), (l)) do not show any deterioration over all the frequency ranges of interest, in the mimicked rainy days. The above experimental results indicate that the superhydrophobic antenna can perform in perfect working conditions in either rainy or sunny environments.

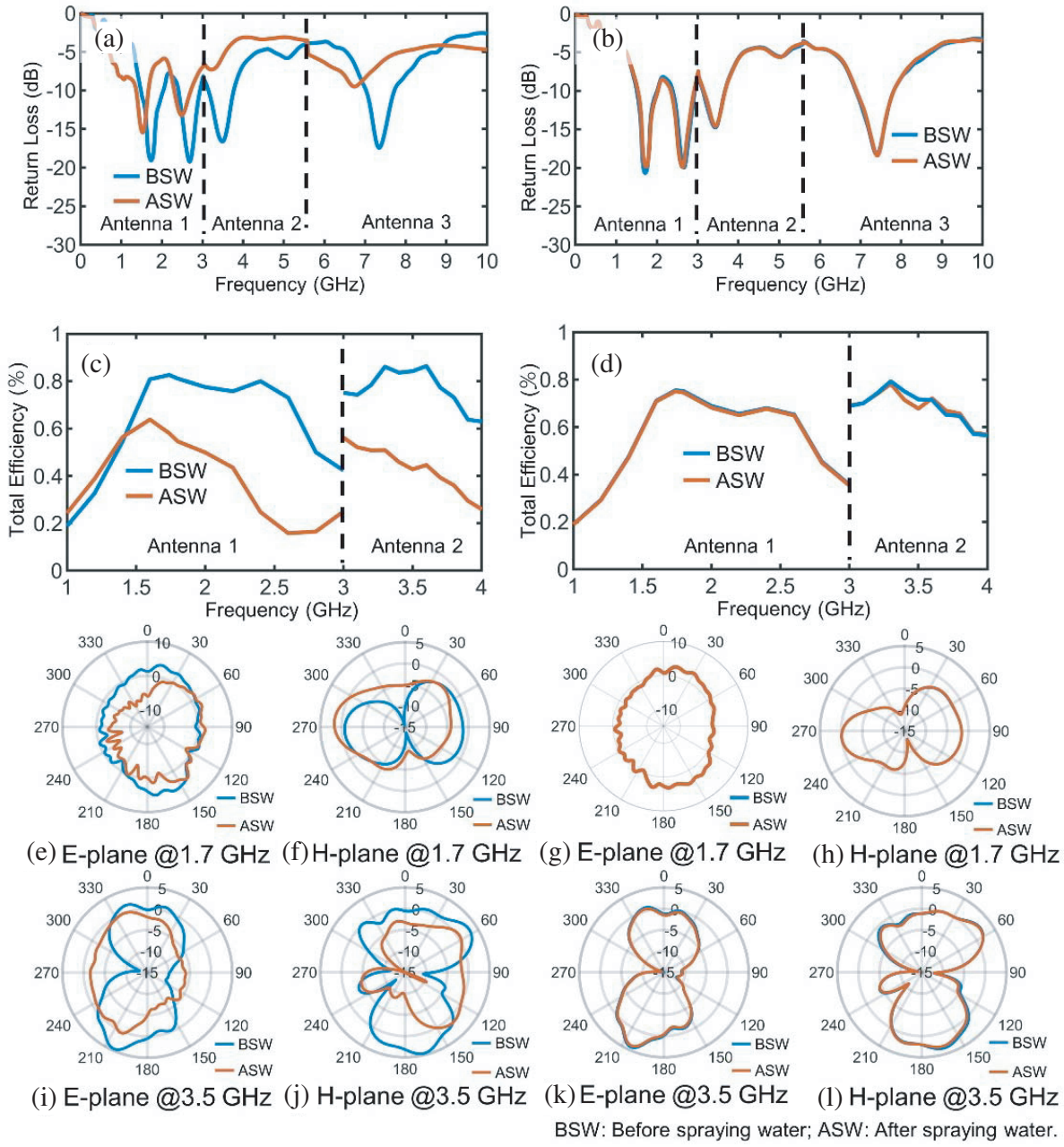

Figure 6. The antenna performance before spraying water (blue curves) and after spraying water (red curves). (a) The return loss of conventional PCB antenna. (b) The return loss of self-superhydrophobic antenna. (c) Total efficiency of conventional PCB antenna. (d) Total efficiency of self-superhydrophobic antenna. (e), (f) *E*-plane and *H*-plane radiation pattern of conventional PCB Antenna 1. (g), (h) *E*-plane and *H*-plane radiation pattern of self-superhydrophobic Antenna 1. (i), (j) *E*-plane and *H*-plane radiation pattern of conventional PCB Antenna 2. (k), (l) *E*-plane and *H*-plane radiation pattern of self-superhydrophobic Antenna 2. Due to the limitation of Satimo antenna test system, the efficiency and radiation pattern of Antenna 3 is not measured in the experiment.

3. CONCLUSION

We developed a self-superhydrophobic antenna in this work by directly writing a hydrophobic microstructure on the surface of conventional PCB antenna. Compared to conventional PCB antennas, the self-superhydrophobic antennas can maintain predefined working status in rainy days without any sacrifice of critical antenna performance, e.g., return loss, efficiency and radiation pattern. The self-superhydrophobic architecture, without the necessity of additional radomes or waterproof coatings, matches the requirement of multiband integration for future communication systems that covers the bands from sub-6G to higher frequencies. Furthermore, it is important to note that the proposed laser-direct-writing treatment is compatible with conventional printed-circuit-board technology.

This work has a wide range of potential applications [41–43], particularly for some antennas that operate in harsh conditions, such as climate monitoring and maritime communications. The proposed technique offers a new research area on the combination of ultrafast laser technology with unique electromagnetic device realization.

ACKNOWLEDGMENT

This work at Jilin University was sponsored by the National Natural Science Foundation of China (NSFC) Grant Nos. 62175083, 61935015, 62275100 and 61905087. This work was also supported by Fundamental Research Funds for the Central Universities.

REFERENCES

1. Vukicevic, A., F. Rachidi, M. Rubinstein, and S. V. Tkachenko, "On the evaluation of antenna-mode currents along transmission lines," *IEEE T. Electromagn. C.*, Vol. 48, 693, 2006.
2. Qin, Y. F. and D. H. Werner, "Dual-band omnidirectional/unidirectional patch antenna based on multiconductor transmission line theory," *IEEE International Symposium on Antennas and Propagation*, 17280945, 2017.
3. Morozov, V. M. and V. I. Magro, "Method of analysis of antennas and transmission lines," *6th International Conference on Antenna Theory and Techniques*, 9704288, 2007.
4. Frank, G., "An insightful derivation of transmission line equations including electromagnetic field-coupling," *2018 International Symposium on Electromagnetic Compatibility*, 18149739, 2018.
5. Gronwald, F., J. Nitsch, and S. Tkachenko, "Generalized transmission line theory as an antenna theory for EMC analysis," *Electr. Eng.*, Vol. 93, 147, 2011.
6. Lau, B. K., J. B. Andersen, G. Kristensson, and A. F. Molisch, "Impact of matching network on bandwidth of compact antenna arrays," *IEEE T. Antenn. Propag.*, Vol. 54, 3225, 2006.
7. Fei, Y., Y. Fan, B. K. Lau, and J. S. Thompson, "Optimal singleport matching impedance for capacity maximization in compact MIMO arrays," *IEEE T. Antenn. Propag.*, Vol. 56, 3566, 2008.
8. Tsen, W. F. and H. J. Li, "Uncoupled impedance matching for capacity maximization of compact MIMO arrays," *IEEE Antenn. Wirel. Pr.*, Vol. 8, 1295, 2009.
9. Allen, J. C., J. Rockaway, and D. Arceo, "Wideband multiport matching phase I: Single-feed multiport antennas," Tech. Rep. SSC/SD-TR-1972, Space and Naval Warfare Systems Center, 2008.
10. Skirelis, J., A. Patlins, N. Kunicina, A. Romanovs, and A. Zabasta, "Wireless sensor networks: Towards resilience against weather-based disruptions," *Electr. Control. Commu.*, Vol. 15, 79, 2019.
11. Li, M., W. J. Lou, and K. Ren, "Data security and privacy in wireless body area networks," *IEEE Wirel. Commun.*, Vol. 17, 51, 2010.
12. John, F. F., J. J. Ma, and L. Moeller, "Review of weather impact on outdoor terahertz wireless communication links," *Nano Commun. Netw.*, Vol. 10, 13, 2016.
13. Wing, S., "Mobile and wireless communication: Space weather threats, forecasts, and risk management," *IT Prof.*, Vol. 14, 40, 2012.

14. Rashed, A. N. Z. and M. M. E. El-Halawany, "Transmission characteristics evaluation under bad weather conditions in optical wireless links with different optical transmission window," *Wireless Pers. Commun.*, Vol. 71, 1577, 2013.
15. Orta, R., R. Tascone, and R. Zich, "Performance degradation of dielectric radome covered antennas," *IEEE T. Antenn. Propag.*, Vol. 36, 1707, 1988.
16. Du, Y. W., *Telecommunications Design Method of the Radome*, National Defense Industry Press, China, 1993.
17. Li, P., W. Y. Xu, and L. W. Song, "A novel compensation strategy for the radiation characteristics of large dielectric radomes based on phase modification," *IEEE Antenn. Wirel. Pr.*, Vol. 15, 1044, 2016.
18. Li, Y. R., X. Jin, W. Li, J. R. Niu, X. Han, X. F. Yang, W. Y. Wang, T. Lin, and Z. T. Zhu, "Biomimetic hydrophilic foam with micro/nano-scale porous hydrophobic surface for highly efficient solar-driven vapor generation," *Sci. China Mater.*, Vol. 65, 1057, 2021.
19. Costa, F. and A. Monorchio, "A frequency selective radome with wideband absorbing properties," *IEEE T. Antenn. Propag.*, Vol. 60, 2740, 2012.
20. Chen, H. Y., X. Y. Hou, and L. J. Den, "Design of frequency-selective surfaces radome for a planar slotted waveguide antenna," *IEEE Antenn. Wirel. Pr.*, Vol. 8, 1231, 2009.
21. Zhou, H., S. B. Qu, B. Q. Lin, and P. Bai, "Filter-antenna consisting of conical FSS radome and monopole antenna," *IEEE T. Antenn. Propag.*, Vol. 60, 3040, 2012.
22. Ye, D. X., Z. Wang, Z. Y. Wang, K. W. Xu, B. Zhang, J. T. Huangfu, C. Z. Li, and L. X. Ran, "Towards experimental perfectly-matched layerswith ultra-thin metamaterial surfaces," *IEEE T. Antenn. Propag.*, Vol. 60, 5164, 2012.
23. Fang, Y., G. Sun, Y. H. Bi, and H. Zhi, "Multiple-dimensional micro/nano structural models for hydrophobicity of butterfly wing surfaces and coupling mechanism," *Sci. Bull.*, Vol. 60, 256, 2015.
24. Wang, D. H., Q. Q. Sun, R. H. A. Ras, and X. Deng, "Design of robust superhydrophobic surfaces," *Nature*, Vol. 582, 55, 2020.
25. Zhang, W., Y. L. Wu, J. C. Li, M. M. Zou, and H. Y. Zheng, "UV laser-produced copper micro-mesh with superhydrophobic-oleophilic surface for oil-water separation," *J. Mater. Res. Technol.*, Vol. 15, 5733, 2021.
26. Liu, X. Q., Y. L. Zhang, Q. K. Li, J. X. Zheng, Y. M. Lu, S. Juodkazis, Q. D. Chen, and H. B. Sun,"Biomimetic sapphire windows enabled by inside-out femtosecond laser deep-scribing," *PhotoniX*, Vol. 3, 1, 2022.
27. Lu, Y. M., Y. Z. Duan, X. Q. Liu, Q. D. Chen, and H. B. Sun, "High-quality rapid laser drilling of transparent hard materials," *Opt. Lett.*, Vol. 47, 921, 2022.
28. Hua, J. G., S. Y. Liang, Q. D. Chen, S. Juodkazis, and H. B. Sun, "Free-form micro-optics out of crystals: Femtosecond laser 3D sculpturing," *Adv. Funct. Mate.*, Vol. 32, 2200255, 2022.
29. Liu, Y. Q., J. W. Mao, Z. D. Chen, D. D. Han, Z. Z. Jiao, J. N. Ma, H. B. Jiang, and H. Yang, "Three-dimensional micropatterning of grapheneby femtosecond laser direct writing technology," *Opt. Lett.*, Vol. 45, 1, 2020.
30. Gao, S., Z. Z. Li, Z. Y. Hu, F. Yu, Q. D. Chen, Z. N. Tian, and H. B. Sun, "Diamond optical vortex generator processed byultraviolet femtosecond laser," *Opt. Lett.*, Vol. 50, 9, 2020.
31. Gao, S., S. Y. Yin, Z. X. Liu, Z. D. Zhang, Z. N. Tian, Q. D. Chen, N. K. Chen, and H. B. Sun, "Narrow-linewidth diamond single-photon sources prepared via femtosecond laser," *Appl. Phys. Lett.*, Vol. 120, 023104, 2021.
32. Gao, S., Z. N. Tian, P. Yu, H. Y. Sun, H. Fan, Q. D. Chen, and H. B. Sun, "Deep diamond single-photon sources prepared by a femtosecond laser," *Opt. Lett.*, Vol. 46, 4386, 2021.
33. Liu, X. Q., R. Cheng, J. X. Zheng, S. N. Yang, B. X. Wang, B. F. Bai, Q. D. Chen, and H. B. Sun, "Wear-resistant blazed gratings fabricated by etching-assisted femtosecond laser lithography," *Opt. Lett.*, Vol. 39, 4690, 2021.
34. Li, Z. Z., X. Y. Li, F. Yu, Q. D. Chen, Z. N. Tian, and H. B. Sun, "Circular cross section waveguides processed by multi-foci-shaped femtosecond pulses," *Opt. Lett.*, Vol. 46, 520, 2021.

35. Mao, Y. H., D. Zhao, C. F. Zhang, K. Huang, and Y. L. Chen, "A vacuum ultraviolet laser with a submicrometer spot for spatially resolved photoemission spectroscopy," *Light Sci. Appl.*, Vol. 10, 22, 2021.
36. Xu, S., H. Fan, Z. Z. Li, J. G. Hua, Y. H. Yu, L. Wang, Q. D. Chen, and H. B. Sun, "Ultrafast laser-inscribed nanogratings in sapphire for geometric phase elements," *Opt. Lett.*, Vol. 46, 536, 2021.
37. Liu, X. Q., S. N. Yang, L. Yu, Q. D. Chen, Y. L. Zhang, and H. B. Sun, "Rapid engraving of artificial compound eyes from curved sapphire substrate," *Adv. Funct. Mate.*, Vol. 29, 1900037, 2019.
38. Liu, H. G., W. X. Lin, and M. H. Hong, "Hybrid laser precision engineering of transparent hard materials: Challenges, solutions and applications," *Light Sci. Appl.*, Vol. 10, 162, 2021.
39. Zhao, Y., Y. M. Yang, and H. B. Sun, "Nonlinear meta-optics towards applications," *PhotoniX*, Vol. 2, 3, 2021.
40. Lai, P. T., Z. L. Li, W. Wang, J. Qu, L. W. Wu, Z. Zhu, Y. X. Li, J. H. Shi, et al., "Transmissive 2-bit anisotropic coding metasurface," *Chin. Phys. B*, Vol. 31, 098102, 2022.
41. Dong, G. H., Z. J. Jiang, Y. C. Li, Z. Zhu, Z. H. Liu, J. H. Shi, et al., "Large asymmetric anomalous reflection in bilayer gradient metasurfaces," *Opt. Express*, Vol. 29, 16796, 2021.
42. Xu, W. X., W. J. Li, Z. Q. Jiang, J. L. Liu, J. H. Shi, et al., "Direction-dependent polarization modulation of Cherenkov diffraction radiation based on metasurfaces," *J. Appl. Phys.*, Vol. 132, 113101, 2022.
43. Li, Z. L., W. Wang, S. X. Deng, J. Qu, Y. X. Li, C. Y. Guan, J. H. Shi, et al., "Active beam manipulation and convolution operationin VO2-integrated coding terahertz metasurfaces," *Opt. Lett.*, Vol. 47, 441, 2022.